PERGAMON

International Journal of Solids and Structures 39 (2002) 3079–3104

INTERNATIONAL JOURNAL OF SOLIDS and STRUCTURES

www.elsevier.com/locate/ijsolstr

Theoretical study of formation of pores in elastic solids: particulate composites, rubber toughened polymers, crazing

Klaus P. Herrmann [a,*], Victor G. Oshmyan [b,*]

[a] *Paderborn University, Pohlweg 47-49, D-33098 Paderborn, Germany*

[b] *Institute of Chemical Physics, Russian Academy of Sciences, Kosygin Str. 4, 117977 Moscow, Russia*

Received 7 February 2001; received in revised form 18 October 2001

Abstract

It is difficult to overestimate the multi-functional role and practical meaning of the processes of the formation of pores in solids, especially in polymers and polymer based materials, which are capable to a noticeable plastic deformation. Various mechanisms are responsible for this phenomenon in different systems. Particularly, it is debonding in particulate filled composites, elastomeric inclusions failure in rubber toughened polymers, nucleation of microvoids at defects in glassy polymers. Two main effects of the formation of pores should be underlined. The first is a decrease in the material's stiffness, which is mostly emphasized for composites filled by rigid inclusions. The second is an improvement in the fracture toughness which is widely explored in practice. The nucleation of pores affects the fracture toughness, firstly, absorbing the energy for the new surface formation and, secondly, facilitating of a plastic flow of the basic material. The paper proposed is partly a review of previously obtained results and represents also the novel data and laws. It concerns two aspects of the problem. An analysis of the conditions advantageous for the appearance of a single pore and of the completeness of this event is the first. This part of the paper is mostly a review, but a novel comparable analysis of the regularities of a pore formation by the way of a debonding along the surfaces of rigid particles in particulate filled composites and caused by a failure of rubbery inclusions will be presented. The second aspect of the problem is a spatial cooperation in the nucleation of pores. Some results in this field also have been obtained previously. However, the corresponding part of the paper mostly represents new data as well as a new analysis. Three types of systems will be analyzed from the cooperation point of view: particulate filled composites, rubber toughened plastics and homogeneous polymers for which a formation of micropores in a diffuse or a cooperative manner is a well known phenomenon named as crazing. Certain corrections of the previous conclusions concerning the cooperation arising during the failure of rubbery particles have been performed. Furthermore, the angles of the disposition of porous zones will be estimated. In addition, it will be shown that the conditions advantageous for an individual cavitation as well as the laws of a diffuse or cooperative proceeding of the multiple crazing are qualitatively the same. However, the different features will also be stated.

Keywords: Microporous zones; Cavitation mechanisms; Particle size distribution; Deformation diagrams; Particulate composites; Rubber toughened polymers

* Corresponding authors. Fax: +49-5251-603-483 (K.P. Herrmann), +7-095-137-82-84 (V.G. Oshmyan).

E-mail addresses: jherr1@ltm.uni-paderborn.de (K.P. Herrmann), oshmyan@chph.ras.ru (V.G. Oshmyan).

0020-7683/02/$ - see front matter
PII: S0020-7683(01)00283-9

Nomenclature

(x_1, x_2, x_3) Cartesian coordinates
(r, θ, φ) spherical coordinates
u_i displacement components
ε_{ij} strain tensor's components
ε macroscopic strain at tension
ε_{st}^{u} macroscopic uniaxial strain value corresponded to a start of uncorrelated cavitation
ε_{st}^{c} macroscopic uniaxial strain value corresponded to a start of correlated cavitation
σ_{ij} stress tensor's components
$\sigma_{ij}^{(\cdot)}$ stress tensor's components in matrix (m) or inclusion (i)
σ macroscopic tension stress
σ_c external tension stress sufficient for cavitation
$C_{ijkl}^{(\cdot)}$ elasticity tensor's components in matrix (m) or inclusion (i)
$K^{(\cdot)}$, $\mu^{(\cdot)}$, $E^{(\cdot)}$, $\nu^{(\cdot)}$ bulk, shear, Young's moduli and Poisson ratio of matrix (m) or inclusion (i)
Φ initial volume fraction of inclusions
x volume fraction of pores, i.e. of cavitated inclusions, $0 \leqslant x \leqslant \Phi$
S specific pores' surface per a unit composite volume
K, μ, E, ν or
K^+, μ^+, E^+, ν^+ effective bulk, shear, Young's moduli and Poisson ratio of a composite without pores
$\hat{K}$, $\hat{\mu}$, $\hat{E}$, $\hat{\nu}$ effective bulk, shear, Young's moduli and Poisson ratio of a composite with partly cavitated inclusions: uncorrelated mechanism of cavitation is supposed
K^-, μ^-, E^-, ν^- effective bulk, shear, Young's moduli and Poisson ratio of a composite with completely cavitated inclusions
$\hat{J}_{ijkl}$ effective compliance tensor of the composite with partly cavitated inclusions: uncorrelated mechanism of cavitation is supposed
J_{ijkl}^{+} effective compliance tensor of the composite without pores
J_{ijkl}^{-} effective compliance tensor of the composite with completely cavitated inclusions
$\hat{J}_{ijkl}^{c}(\varphi)$ effective compliance tensor of the composite with partly cavitated inclusions: correlated mechanism of cavitation is supposed
φ the slope of microporous zone formed by the way of correlated cavitation to the direction, which is transverse to the tension axis
W specific (per unit volume) work of deformation
U_e, U_S specific elastic and surface energies
γ specific surface energy density referred to whether inclusion–matrix or pore–inclusion interface
$\bar{\gamma}$ reduced specific surface energy density
Γ_p pore–matrix interface
Γ_i inclusion–matrix interface
Γ_S external boundary of the composite sphere
r_p, r_i, r_S radii of pore, inclusion and composite sphere (Fig. 1), respectively
R_p, R_i, R_S dimensionless radii of pore, inclusion and composite sphere
ψ debonding angle

1. Introduction

The formation of pores in homogeneous as well as in heterogeneous solids essentially determines the deformation and the fracture properties of a material. It can be caused by various reasons. Particularly, debonding along the surfaces of hard inclusions is the most efficient mechanism for particulate filled polymers. Further, cohesive failure of elastomeric particles, i.e. cohesive failure of rubber phase, causes a nucleation of pores in rubbery toughened materials. Moreover, diffuse or cooperative crazing in homogeneous glassy polymers is a well-known phenomenon, which accompanies deformation, plastic flow and fracture. Corresponding microporous zones are often called as silver cracks.

It is undoubtedly shown (see Knunyantz et al., 1983, 1986; Dekkers and Heikens, 1986; Vollenberg and Heikens, 1989; Vollenberg et al., 1989; Berlin et al., 1990, 1992; Gorbunova et al., 1990; Fu and Wang, 1993; Fu et al., 1993; Michler, 1993; Pukansky et al., 1994, 1995; Bazhenov, 1995; Kim et al., 1996; Dubnikova et al., 1997a,b; Dubnikova and Oshmyan, 1998; Muravin and Oshmyan, 1999) that the values of the debonding stress and of the fraction of pores created strongly affect the mechanisms and parameters of the deformation and fracture of particulate filled composites. In particular, an increase in the adhesive strength causes a decrease in the pores fractions, which results in an increase in the elastic moduli, the yield stresses and provides brittleness of the material.

Modification of brittle polymers (e.g. polystyrene, polycarbonate, epoxy) by rubber is an efficient way for material toughening (Bucknall, 1977; Paul and Newman, 1978; Wu, 1985, 1988; Ishikawa, 1995; Ishikawa and Chiba, 1990; Ishikawa et al., 1996; D'Orasio et al., 1991; Kikuchi et al., 1991, 1992; Kozii and Rosenberg, 1992; Michler, 1993; Inoue and Suzuki, 1994, 1995; Kim et al., 1996). It is undoubtedly shown that failure of elastomeric inclusions essentially promotes the toughening.

A diffuse (delocalized) or a cooperative (localized) accumulation of microvoids in glassy polymers named as crazing is well-known and widely discussed in the literature and therefore it does not make a sense to give any special references. The significance of this phenomenon is determined by the fact that crazes (silver cracks) are the only source for a plastic deformation of such materials: contrary to bulk polymer thin polymer layers in microporous zones are capable to large non-destructive deformations.

Nucleation, accumulation, growth and confluence of pores in plastic materials is one of the most probable and acceptable mechanism of ductile fracture. A corresponding theoretical model was proposed by McClintock et al. (1966, 1968). Further, the creation of a new portion of a free surface as a result of any kind of a microfracture event absorbs a certain portion of the work applied and thereby serves as a channel of energy dissipation. At least, the appearance of pores essentially changes the deformation and fracture abilities of the host. Particularly, it was already shown that very thin films can exhibit large plastic flow in contrast to the bulk material. On the other side, the formation of large pores promotes the stabilization of silver cracks and also of multiple crazing.

So, the study of the regularities of pores formation both in heterogeneous and homogeneous materials is very important for the understanding of the associated laws which describe the phenomena of the deformation, flow and fracture. It has a special meaning also for the optimization of the corresponding characteristics. Three systems are considered. Particulate filled composites are the first. Debonding along the interfaces of rigid inclusions is assumed to be responsible for the pores formation. Rubber toughened polymers are the second. It is supposed that cohesive failure of elastomeric inclusions is the main mechanism of the microfracture event. Homogeneous glassy polymers are the third. A model similar to that for a rubber toughened polymer has been developed in this case: the elastomeric inclusion is formally replaced by the host including defects which cause the "inclusion's" fracture.

Two aspects of the microfracture process can be obviously stated. The first one is the nucleation of individual pores (primary portion) without any account of a mutual influence. The value of the macroscopic stress sufficient for cavitation, σ_c, and the size of the pores are of special interest. A brief review of the results of corresponding and rather comprehensive theoretical investigations, particularly performed by the

authors has been given in the paper. The main attention has been paid to a comparison of two mechanisms: debonding along the surface of a hard particle in a particulate filled composite and elastomeric inclusion failure in a rubber toughened polymer.

The diffuse (uncorrelated) or cooperative (correlated) development of different microfracture events is the second side of the problem. The formation of crazes or craze-like microporous zones has been observed and reported by many authors (see Bucknall, 1977; Paul and Newman, 1978; Michler, 1993; Lazzery and Bucknall, 1995; Kim et al., 1996; Dubnikova et al., 1997a,b; Dubnikova and Oshmyan, 1998). However, only preliminary theoretical simulations of the phenomenon at the elastic stage of deformation have been performed recently by us (Dubnikova et al., 1997a,b; Herrmann and Oshmyan, 1997; Oshmyan and Muravin, 1997). The development and correction of corresponding models as well as a comparable analysis of the phenomenon for three systems is another goal of the paper. Particularly, the slope of a microporous zone with respect to a deformation axis has been estimated. Such a kind of estimation was previously given by Lazzery and Bucknall (1995) for the case of a toughened plastic. However, it was done as for a shear band in a dilatation sensible porous media. Certainly, this approach can be used for the angle of highly deformed zones in already porous media or for zones formed during yielding but not for the elastic stage of a deformation.

The paper is organized as follows. Composite mechanics models used in the further simulations are described in Section 2. Approaches and results for an estimation of the cavitation stress as well as of the pore size are given and discussed in Section 3. The simulation of uncorrelated or correlated mechanisms of an accumulation of voids as well as of the transition between these mechanisms forms the subject of Section 4.

2. Composite mechanics models

Two different approaches applied in modern composite mechanics are used in the paper. The so-called composite sphere model is better adapted for a description of an individual cavitation. Two reasons justify a corresponding choice. Firstly, numerical methods can be applied for the solution of a basic cell-problem, which is impossible for any self-consistent approach. Such a necessity appears in the case of an interfacial crack along the surface of a hard inclusion. Secondly, it will be shown below that a composite sphere model admits a non-cumbrous analytical solution for a three- (multi-)phase composite which in fact is a system consisting of a host with an inclusion and pore inside in the case of an arising failure of an elastomeric particle in a rubber toughened polymer.

The differential self-consistent approach is better adapted for a simulation of the process of an accumulation of pores because its basic idea consists in a sequent addition of new small portions of inhomogeneities into an effectively homogeneous elastic continuum.

2.1. Composite sphere model

The structural assumptions of a composite sphere model proposed by Hashin (1962) are illustrated in Fig. 1a.

The inclusions are supposed to be of the same (spherical) shape but of different size, and they are distributed in space in such a way that their shells of radii r_s which are proportional to the radii r_i of the inclusions can only touch each other without intersections. A natural approximation of the stress–strain state (SSS) in a composite by an identical SSS in every structural cell (Fig. 1b or 1c) is very convenient and also sufficiently exact. Really, it reduces the problem of the SSS calculation to the solution of a boundary value problem within a single representative cell. The arbitrary type of the triangle of touching cells provides the following linear conditions for the displacement field on the boundary Γ_s of the cell:

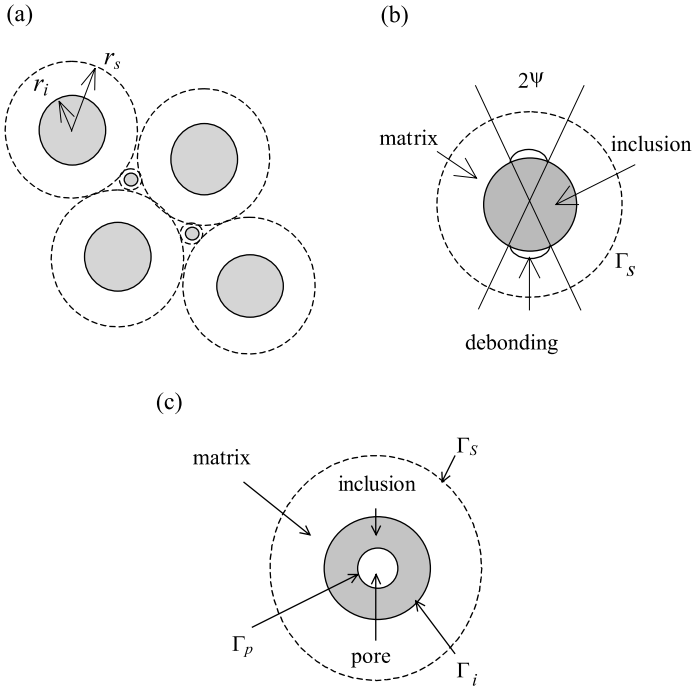

Fig. 1. Scheme of the composite sphere structural model for a composite (a) and its representative spherical shells for the problems of particle debonding (b) and inclusion failure (c).

$$u_i|_{\Gamma_s} = \sum_j \varepsilon_{ij} x_j, \tag{1}$$

where ε_{ij} are the macro strain tensor components.

Furthermore, the central symmetry of the cell structure (Fig. 1) and of the boundary conditions (1) provides the equality of the stresses in the touching points of neighboring cells and hence, delivers the equilibrium of the system.

For the simulation of the debonding process in a particulate filled composite caused by a uniaxial tension the following boundary value problem is stated and solved for the representative cell of Fig. 1b. Symmetric debonding sectors, which surround the poles of a rigid inclusion by forming a debonding angle ψ are supposed to be given. It means that the host is stress-free or satisfies slipping conditions on the debonded part of the interface and zero values for the displacement vector at the bonded area. A corresponding boundary value problem has been numerically solved by the finite element method (FEM). All the details of the formulation and the solution of the boundary value problem can be found in our previous publications: Berlin et al. (1991, 1992), Zhuk et al. (1993a,b, 1994).

A pore is supposed to be spherical and concentric to a spherical inclusion if a mechanism of an inclusion's cohesive failure for cavitation is accepted (Fig. 1c). Then three phases (pore, inclusion and matrix) and two interfaces (pore–inclusion, Γ_p, and inclusion–matrix, Γ_i) appear.

The equilibrium equations

$$\frac{\partial \sigma_{ij}}{\partial x_j} = 0 \tag{2a}$$

together with the continuity conditions

$$\sigma_{rr}^{(\mathrm{m})}\big|_{\Gamma_\mathrm{i}} = \sigma_{rr}^{(\mathrm{i})}\big|_{\Gamma_\mathrm{i}}, \quad \sigma_{r\theta}^{(\mathrm{m})}\Big|_{\Gamma_\mathrm{i}} = \sigma_{r\theta}^{(\mathrm{i})}\Big|_{\Gamma_\mathrm{i}} \tag{2b}$$

at the interface Γ_i, the boundary conditions

$$\sigma_{rr}^{(\mathrm{i})}\big|_{\Gamma_\mathrm{p}} = 0, \quad \sigma_{r\theta}^{(\mathrm{i})}\Big|_{\Gamma_\mathrm{p}} = 0 \tag{2c}$$

at the stress-free boundary Γ_p, and the Eq. (1) form together with the constitutive equations

$$\sigma_{ij} = C_{ijkl}^{(\cdot)}\varepsilon_{kl} \tag{3}$$

(superscript $(\cdot)$ defines a region of matrix (m) or inclusion (i)) an appropriate boundary value problem for a representative cell (Fig. 1c). In a case of isotropic phases the solution of the problem (1)–(3) can be found in spherical coordinates (r, θ, φ) in the form:

$$u_r^{(\cdot)} = D_1^{(\cdot)} r + \frac{D_2^{(\cdot)}}{r^2}, \quad u_\theta^{(\cdot)} = u_\varphi^{(\cdot)} = 0, \tag{4a}$$

for a dilatation,

$$\|\varepsilon_{ij}\| = \delta \begin{pmatrix} 1 & 0 & 0 \\ 0 & 1 & 0 \\ 0 & 0 & 1 \end{pmatrix}$$

and

$$\begin{aligned} u_r^{(\cdot)} &= \left(S_1^{(\cdot)} r + \frac{S_2^{(\cdot)}}{r^2} + S_3^{(\cdot)} r^3 + \frac{S_4^{(\cdot)}}{r^4} \right) \cos 2\theta, \\ u_\theta^{(\cdot)} &= -\left(3S_1^{(\cdot)} r + \frac{6\left(1-2\nu^{(\cdot)}\right)}{5-4\nu^{(\cdot)}} \frac{S_2^{(\cdot)}}{r^2} + \frac{7-4\nu^{(\cdot)}}{2\nu^{(\cdot)}} S_3^{(\cdot)} r^3 - 2\frac{S_4^{(\cdot)}}{r^4} \right) \sin 2\theta, \\ u_\varphi^{(\cdot)} &= 0, \end{aligned} \tag{4b}$$

for a x_1-symmetrical macroscopic shear, $\left\|\varepsilon_{ij}\right\| = \gamma \begin{pmatrix} 2 & 0 & 0 \\ 0 & -1 & 0 \\ 0 & 0 & -1 \end{pmatrix}$, where the D_i $(i = 1, 2)$ and S_i $(i = 1\text{–}4)$ are constants which can be determined by using the boundary and continuity conditions (2b) and (2c). It is sensible to note that analytical solutions can be found in the form (4a) and (4b) for a multi-phase composite sphere of an arbitrary number, n, of concentric spherical shells.

2.2. Differential self-consistent model

A criterion for the uncorrelated or correlated occurrence of the formation of pores is based on the description of their gradual accumulation. A differential self-consistent model of Vavakin and Salganik (1975) suggests a gradual incorporation of new small portions of inclusions into an effectively homogeneous medium, which has been formed at previous steps (see the sketch in Fig. 2). Thereby the differential self-consistent model is mostly adapted for the simulation proposed.

Asymptotic analytical formulas for the effective bulk, K, and shear, μ, moduli of an isotropic elastic continuum characterized by the moduli $K^{(\mathrm{m})}$, $\mu^{(\mathrm{m})}$, and filled by an infinitesimal small portion Φ of isotropic spherical inclusions with the moduli $K^{(\mathrm{f})}$, $\mu^{(\mathrm{f})}$

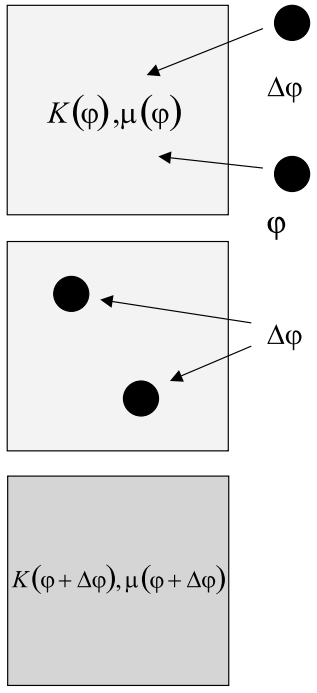

Fig. 2. Sketch of the differential self-consistent model.

$$K = K^{(m)} + \Phi \frac{\left(3K^{(m)} + 4\mu^{(m)}\right)\left(K^{(f)} - K^{(m)}\right)}{3K^{(f)} + 4\mu^{(m)}}, \tag{5a}$$

$$\mu = \mu^{(m)} + \Phi \frac{5\mu^{(m)}\left(3K^{(m)} + 4\mu^{(m)}\right)\left(\mu^{(f)} - \mu^{(m)}\right)}{6\mu^{(f)}(K^{(m)} + 2\mu^{(m)}) + \mu^{(m)}(9K^{(m)} + 8\mu^{(m)})} \tag{5b}$$

are well known and can be found almost in every book on mechanics of composite materials, see e.g. Christensen (1979).

An idea of a gradual addition of a small new portion of particles into an effectively homogeneous medium admits the application of Eqs. (5a) and (5b) with a replacement of Φ by $\Delta\varphi$, K_m, μ_m, by $K(\varphi)$, $\mu(\varphi)$, K, μ, by $K(\varphi + \Delta\varphi)$, $\mu(\varphi + \Delta\varphi)$, and thereby the reduction of the problem of a calculation of effective moduli to the solution of a system of ordinary differential equations

$$\frac{dK}{d\varphi} = \frac{(3K + 4\mu)\left(K^{(f)} - K\right)}{3K^{(f)} + 4\mu}, \tag{6a}$$

$$\frac{d\mu}{d\varphi} = \frac{5\mu(3K + 4\mu)\left(\mu^{(f)} - \mu\right)}{6\mu^{(f)}(K + 2\mu) + \mu(9K + 8\mu)} \tag{6b}$$

with natural initial conditions

$$K(0) = K^{(m)}, \quad \mu(0) = \mu^{(m)}. \tag{6c}$$

Besides, the parameter φ is linked with the filler fraction Φ by the relation:

$$d\varphi = \frac{d\Phi}{1-\Phi}, \quad \varphi = \ln\frac{1}{1-\Phi}. \tag{6d}$$

Nevertheless, a numerical integration of the Cauchy problem (6a)–(6d) does not meet any difficulties in the general case, it admits simple analytical solutions for certain particular cases.

2.2.1. Rigid inclusions

In the limit $K^{(f)} \to \infty$, $\mu^{(f)} \to \infty$ the system of differential equations can be reduced to one equation for the ratio, $u = K/\mu$,

$$\frac{du}{d\varphi} = \frac{(4+3u)(4-3u)}{6(u+2)} \tag{7a}$$

or for the Poisson ratio, v,

$$\frac{dv}{d\varphi} = \frac{3(1-2v)(1-5v)(1-v)}{2(4-5v)}, \tag{7b}$$

which, in turn, admits the following analytical solution:

$$1-\Phi = \sqrt[6]{\frac{(4-3u)^5(4+3u^{(m)})}{(4-3u^{(m)})^5(4+3u)}}, \tag{8a}$$

$$K = K^{(m)}\frac{u}{u^{(m)}}\sqrt[3]{\left(\frac{4-3u^{(m)}}{4-3u}\right)^5}, \tag{8b}$$

$$\mu = \mu^{(m)}\sqrt[3]{\left(\frac{4-3u^{(m)}}{4-3u}\right)^5}. \tag{8c}$$

Eq. (7b) has a stable stationary point $v = 0.2$. So, in case of $v^{(m)} = 0.2$ the solution of Eqs. (6a)–(6d) is of the most simple form:

$$\mu = \mu^{(m)}(1-\Phi)^{-2}, \quad K = K^{(m)}(1-\Phi)^{-2}, \quad E = E^{(m)}(1-\Phi)^{-2} \tag{8d}$$

(herein and further E is used as a notation for Young's modulus).

2.2.2. Pores

A reduction of Eqs. (6a) and (6b) to a single equation for each of the ratio u and v, respectively, can also be performed for the opposite limit of a pore: $K^{(f)} \to 0$, $\mu^{(f)} \to 0$:

$$\frac{du}{d\varphi} = \frac{3u(4+3u)(4-3u)}{4(8+9u)}, \tag{9a}$$

$$\frac{dv}{d\varphi} = \frac{3(1+v)(1-5v)(1-v)}{2(7-5v)}. \tag{9b}$$

Eqs. (6a)–(6d) can be resolved in an implicit analytical form using the Eq. (9a) for the ratio:

$$1-\Phi = \sqrt[6]{\frac{(4-3u)^5\left(u^{(m)}\right)^4\left(4+3u^{(m)}\right)}{\left(4-3u^{(m)}\right)^5u^4(4+3u)}}, \tag{10a}$$

$$K = K^{(m)} \sqrt[3]{\frac{(4-3u)^5 (u^{(m)})^2}{(4-3u^{(m)})^5 u^2}}, \tag{10b}$$

$$\mu = \mu^{(m)} \sqrt[3]{\left(\frac{(4-3u)u^{(m)}}{(4-3u^{(m)})u} \right)^5}. \tag{10c}$$

Similarly to the case of a rigid particle, $v = 0.2$ is also a stable stationary point for Eq. (9b). Thus, if $v^{(m)} = 0.2$ holds true, we obtain a very simple explicit formula:

$$\mu = \mu^{(m)}(1-\Phi)^2, \quad K = K^{(m)}(1-\Phi)^2, \quad E = E^{(m)}(1-\Phi)^2. \tag{10d}$$

2.2.3. Elastomeric inclusions

We suggest for an elastomer $K^{(f)} = K^{(m)}$, which in connection with the inequality $\mu^{(f)} \ll \mu^{(m)}$ reflects rather precisely a realistic relation for rubber and a thermoset or a thermoplastic polymer. The first relation provides the Φ-independence of the bulk modulus

$$K \equiv K^{(f)} = K^{(m)} \tag{11a}$$

and, hence, an independent equation (6b) for the shear modulus. It also admits an implicit analytical solution and therefore in connection with Eq. (11a) follows:

$$1 - \Phi = \frac{\mu - \mu^{(f)}}{\mu^{(m)} - \mu^{(f)}} \sqrt[5]{\frac{(\mu^{(m)})^2 (3K + 4\mu^{(m)})}{\mu^2 (3K + 4\mu)}}, \tag{11b}$$

$$E = \frac{18K\mu}{6K + 2\mu}. \tag{11c}$$

Obviously, the solution (11a)–(11c) is valid not only for a soft inclusion, but also for an arbitrary value of $\mu^{(f)}$.

3. Regularities of an individual cavitation

A complete review of the approaches for a description of a cavitation is not a goal of this paper. It can be found in publications by Berlin et al. (1991, 1992), Zhuk et al. (1993a,b, 1994), Herrmann and Oshmyan (1997), Lazzery and Bucknall (1995). We are going only to mention three approaches, which are based on the conditions of a propagation of a certain microscopic defect and which formed sources for our study.

Toya (1974) used complex potentials for an analytical solution of a 2D problem for the SSS in an infinite elastic continuum with a single circular rigid inclusion having a crack at the interface. Certainly, his solution can be applied for a description of a crack propagation, however, the following objections and restrictions are seen for it. Firstly, his solution can be applied only in the limit of a small, but not arbitrary filler fraction. Secondly, Toya's solution is applicable only in a case of a sufficiently small defect when the crack surfaces are stress-free. The third objection is general for any problem in an interfacial crack analysis: oscillations occur in the neighborhood of a crack tip and in principle a more rigorous analysis should be performed.

Gent (1984) simulated the propagation of a sector-shaped interfacial crack along the surface of a spherical inclusion without the solution of any elasticity problem by estimating the elastic energy release by means of a value for an unloaded volume. Gent's estimation was surprisingly precise, although it is restricted by a small concentration limit.

Lazzery and Bucknall (1995) analytically solved an elasticity problem for a spherical pore surrounded by a concentric spherical shell of an inclusion in an infinite solid simulating by the way a rubber particle failure. A case of a single shell in an infinite matrix also corresponds to a small concentration limit.

The authors of this paper solved similar to Gent (1984) and Lazzery and Bucknall (1995) elasticity problems for the debonding of rigid particles and the failure of elastomeric inclusions by using the composite sphere model described in the previous section. This method allows a generalization of the analysis also to an arbitrary filler fraction.

An elasticity problem for a representative cell of a composite sphere model was solved numerically by the FEM for the debonding phenomenon (Berlin et al., 1991, 1992; Zhuk et al., 1993a,b, 1994) and analytically for the failure of elastomeric inclusions (Herrmann and Oshmyan, 1997). Various additional factors have been studied for the debonding problem in particulate filled composites. Particularly, thermal or chemical contraction, and finite friction between exfoliated surfaces were accounted (Zhuk et al., 1993a,b). The problem of an interfacial crack deviating into a matrix material was studied (Zhuk et al., 1993a,b). The details can be found in corresponding publications. Here we would like to describe only a general approach and to compare the results obtained for a basic case of debonding (without any contraction, friction or crack deviation) with those obtained for the elastomeric inclusions failure.

A general criterion of linear fracture mechanics is applied for a condition advantageous for a formation of a pore:

$$\mathrm{d}U_{\mathrm{e}} \geqslant \mathrm{d}U_{\mathrm{S}}, \tag{12}$$

where $\mathrm{d}U_{\mathrm{e}}$ and $\mathrm{d}U_{\mathrm{S}}$ are increments of the elastic and surface energy, respectively, caused by a defect growth. It is convenient to refer both of the quantities to the unit volume. Let us also restrict the analysis to the case of a uniaxial macroscopic tension by a stress σ. Then the left side of Eq. (12) can be expressed as

$$U_{\mathrm{e}} = \frac{\sigma^2}{2E} = \frac{\sigma^2}{E^{(\mathrm{m})}} U_{\mathrm{e}}^0, \tag{13}$$

where E and $E^{(\mathrm{m})}$ are the composite and matrix Young's moduli, and U_{e}^0 the elastic energy density for a composite with a matrix of unit Young's modulus caused by a unit stress.

In order to clarify the further analysis it makes sense to use dimensionless radii, which will be denoted by capital letters in contrast to the absolute radii values denoted by small letters:

$$R_{\mathrm{i}} = 1, \;\; R_{\mathrm{S}} = \frac{1}{\sqrt[3]{\Phi}}, \;\; r_{\mathrm{p}} = R_{\mathrm{p}} r_{\mathrm{i}}, \;\; r_{\mathrm{S}} = R_{\mathrm{S}} r_{\mathrm{i}} = \frac{r_{\mathrm{i}}}{\sqrt[3]{\Phi}}, \tag{14}$$

where the subscripts S, i and p, refers to the cell, the inclusion and the pore radii (Fig. 1b and c), respectively.

The surface energy densities with account of a shell volume can be described by the formulas:

$$U_{\mathrm{S}} = \gamma \frac{4\pi r_{\mathrm{i}}^2 (1 - \cos\psi)}{\frac{4}{3}\pi r_{\mathrm{S}}^3} = 3\gamma \frac{r_{\mathrm{i}}^2 (1 - \cos\psi)}{r_{\mathrm{S}}^3} = 3\gamma \frac{\Phi(1 - \cos\psi)}{r_{\mathrm{i}}}, \tag{15a}$$

$$U_{\mathrm{S}} = 3\gamma \frac{r^2}{r_{\mathrm{S}}^3} = 3\gamma \frac{\Phi R^2}{r_{\mathrm{i}}} \tag{15b}$$

in the cases of an inclusion debonding (Fig. 1b) and failure (Fig. 1c), respectively, where γ is a specific surface energy density.

It is convenient to introduce a reduced specific surface energy density

$$\bar{\gamma} = 3\gamma \frac{E_{\mathrm{m}}}{\sigma^2 r_{\mathrm{i}}} \tag{16}$$

and to rewrite the cavitation criterion (12) in a dimensionless form:

$$\frac{\mathrm{d}U_{\mathrm{e}}^{0}}{\mathrm{d}\psi}\frac{1}{\Phi} \geqslant \bar{\gamma}\sin\psi, \tag{17a}$$

$$\frac{\mathrm{d}U_{\mathrm{e}}^{0}}{\mathrm{d}R}\frac{1}{\Phi} \geqslant 2\bar{\gamma}R, \tag{17b}$$

for an inclusion debonding and a cohesive failure mechanism, respectively.

A comparison of the elastic and surface energy derivatives has been demonstrated in Fig. 3. It can be seen that for an individual cavitation the laws are very similar for both mechanisms. The following features are seen:

(1) The dependencies of the elastic energy derivatives with respect to the relative size of a defect have a bell-shape both for debonding and an elastomeric inclusion failure. Namely, the first derivative vanishes at zero and for the maximum size of a defect and reaches a unique maximum value at about 65–75% and 20–30% of the maximum defect size for a particulate filled composite and a rubber toughened polymer, respectively.

(2) The second derivative of the reduced elastic energy also vanishes at zero defect size, but the third derivative is positive and seems to be independent of the inclusions content Φ. Therefore, the asymptotic

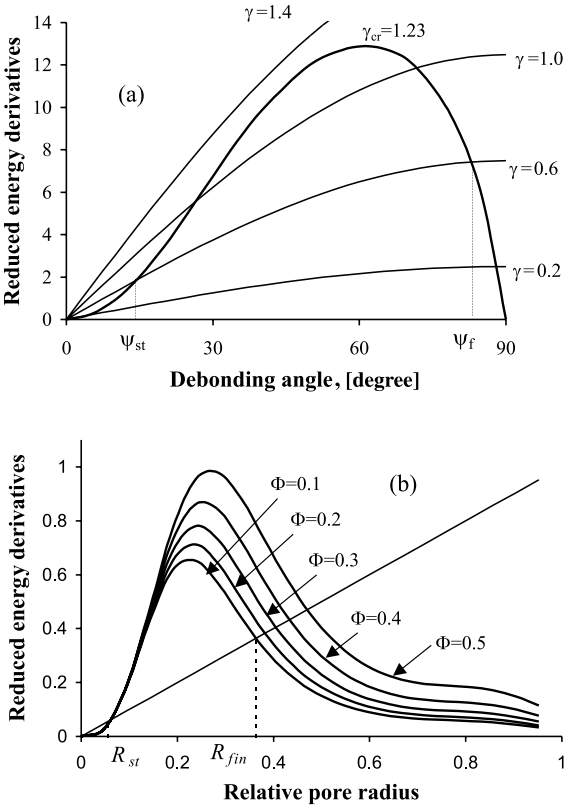

Fig. 3. Elastic (——) and surface (—) energy derivatives via the debonding angle at the interface of a rigid particle (a) and the relative radius of a pore inside of an elastomeric inclusion (b). Figure (a) corresponds to $\Phi = 0.035$ and figure (b) corresponds to $\bar{\gamma} = 0.5$.

behavior of the left-hand side of Eqs. (17a) and (17b) can be described for a small defect size by a second power law:

$$\frac{\mathrm{d}U_{\mathrm{e}}^{0}}{\mathrm{d}\psi}\frac{1}{\Phi}=a_{\mathrm{d}}\psi^{2}, \tag{18a}$$

$$\frac{\mathrm{d}U_{\mathrm{e}}^{0}}{\mathrm{d}R}\frac{1}{\alpha}=a_{\mathrm{f}}R^{2} \tag{18b}$$

with universal constants a_{d}, a_{f} for the debonding of the rigid particle and a failure of an elastomeric inclusion, respectively.

(3) The surface energy derivatives (right-hand sides of Eqs. (17a) and (17b)) are universal monotonously increasing functions of a non-zero slope.

(4) The validity of the previous items generally provides two or zero intersectional points between the bold and normal lines in Fig. 3. That means the existence of a minimum, $\psi_{\mathrm{st}}(R_{\mathrm{st}})$, and a maximum, $\psi_{\mathrm{f}}(R_{\mathrm{f}})$, relative size of a defect, which is capable for propagation. Otherwise in accordance to the criterion accepted, the defect is stable. An important quantitative difference in this aspect should be noted. Different positions of maxima cause different completeness (final size of a pore) of a cavitation. A shift to the right position of a maximum in a case of debonding and a further sharp drop of an elastic energy derivative provide the possibility of an almost complete debonding. On the contrary, in the case of an elastomeric inclusion failure the position of the maximum is shifted to the left and at 50% of a maximum defect size the elastic energy derivatives become small. It means that a complete rupture is not realistic and requires the application of a very intensive load to the material. This difference is caused by the following reason. Young's and shear moduli of an elastomeric inclusion are much lower than those of the matrix and only the bulk modulus values are comparable. Even a small pore inside of an elastomeric particle considerably reduces the bulk deformation of the last. An inclusion shows almost the same behavior as a pore and a further growth of the defect loses its adventure.

(5) The data obtained both for a cavitation in particulate filled composites and in rubber-toughened plastics can be used for the scale factor analysis (dependencies of the cavitation parameters with respect to the absolute inclusion diameter), if the dependence of the initial defect size upon the particle radius is known. This problem requires an additional study, but just now it makes sense to analyze two modeling situations, namely, fixed relative and fixed absolute sizes of the defect. The first one means that $\psi_{\mathrm{st}}(R_{\mathrm{st}})$ and therefore, the left-hand sides of Eqs. (17a) and (17b) at $\psi=\psi_{\mathrm{st}}(R=R_{\mathrm{st}})$ are given and the structure of the right-hand side provides that the cavitation stress, σ_{c}, i.e. the stress sufficient for the pore's formation, is proportional to an inverse square root of the inclusion radius. In the case of a fixed absolute initial defect size, r_{st}, this dependence should by weaker. In the limit of a small defect size one can explore the asymptotic relations (18a) and (18b) in order to derive the independence of the cavitation stress on a characteristic size of the structure.

(6) The model proposed predicts a weak dependence of the cavitation parameters upon the filler fraction (see Fig. 3b) especially for the characterizing start of a cavitation. The final size of the pore shows more sensitivity: the larger the filler fraction is the larger should be the final size of the pore. Certainly, this conclusion is essentially caused due to the structural model. Particularly, a much more strong dependence of the cavitation regularities from the filler fraction had been revealed by Knunyantz and Oshmyan, 1992 for the debonding phenomenon in a particulate filled composite by applying a periodic structural model. One of the most astonishing consequence of a periodic disposition of identical particles is an essential transformation of the shape of a curve reflecting the dependence of an elastic energy derivative on a pore size: unimodal dependence transforms into a bimodal ones at a sufficiently high filler fraction. It means that there appears a so-called "dead zone" for an interfacial crack propagation.

(7) For every given fraction Φ there exists a critical value of the reduced specific surface energy, $\bar{\gamma}_{cr}$, above which bold and normal lines do not intersect. It means that cavitation is forbidden. If one fixes any characteristic size of the structure (inclusion radius, for instance), this feature can be reformulated as the existence of a certain critical cavitation stress, σ_c^{cr}, which drops with r_i accordingly to the inverse square law. The larger Φ is, the larger is $\bar{\gamma}_{cr}$, and the smaller is σ_c^{cr}. However, the corresponding dependencies are rather weak (see Fig. 3).

4. Diffuse and cooperative cavitation mechanisms

The other side of the problem is whether a cavitation proceeds independently on different particles and defects in a sample volume or whether there exists a certain correlation between these microfracture events. Therefore, let us consider a cavitation not as a simultaneous formation of pores but as a gradual accumulation of cavities in a deformation process, which is caused by the work applied. Such a representation was primary proposed by Anderson and Farris (1988) for particulate filled composites and afterwards developed and used for a treatment of their experimental data by Wong and Ait-Kadi (1995). Thereby an uncorrelated debonding mechanism (Fig. 4a) was assumed in this study.

Both cases of uncorrelated and correlated cavitations arising in particulate filled composites due to a debonding (Oshmyan and Muravin, 1997; Dubnikova et al., 1997a,b) as well as in rubber toughened polymers due to an elastomeric inclusions fracture mechanism (Herrmann and Oshmyan, 1997) has recently been simulated by the authors. It was supposed for a correlated mechanism that cavitation occurs in microporous zones, which are transverse to the direction of loading, whenever a complete absence of cavities in the rest area of the material takes place (Fig. 4b).

This investigation will clarify the following problems.

1. A precise and detailed simulation as well as an analysis of stress–strain diagrams by applying a uniaxial tension accompanied by a diffuse and cooperative cavitation has been performed. Moreover, not only the transverse direction of crazes or craze-like regions has been admitted but also an arbitrary slope of the zones (Fig. 4c).
2. The effect of the width as well as of the shape of particle size distributions onto the cavitation mechanism and its development has been studied.
3. The kinetics of a pores accumulation including the start and the finish of the process has been described.

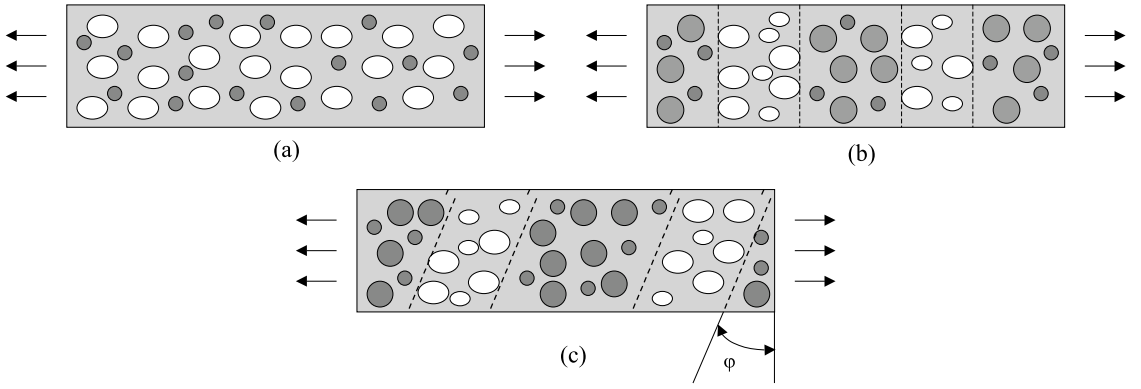

Fig. 4. Schemes of uncorrelated (a) as well as correlated (b), (c) cavitations with a formation of porous zones in the layers transverse to the loading direction (b) and sloped with a certain angle φ to a transverse plane (c).

4. Three systems of great practical interest have been studied, analyzed and compared: particulate filled composites, rubber toughened plastics and homogeneous glassy polymers characterized by localized or delocalized crazing.

4.1. Model of deformation accompanied by a cavitation

The basic idea for the description of a material straining accompanied by a cavitation at an elastic stage of deformation is a link between the strain value, ε, and the volume portion, x, of the particles transformed into pores by a debonding, failure or any other mechanism. This portion can be verified in the interval $0 \leqslant x \leqslant \Phi$ where Φ is a total inclusion volume fraction. The debonding (or failure) of an inclusion is supposed to be complete. So, the pores' volume is equal to an associated inclusions' volume. Therefore, the volume fraction of non-cavitated inclusions can be set to $\Phi - x$. It has been assumed that each pore formed is of the same (spherical) shape and that an inclusion does not anyhow affect a further straining.

Let us denote in the following the effective elastic characteristics of a material, filled by a fraction Φ of inclusions of which a portion x was transformed into pores, as

$$\hat{K}(\Phi,x),\ \ \hat{\mu}(\Phi,x),\ \ \hat{E}(\Phi,x),\ \ \hat{u}(\Phi,x),\ \ \hat{\nu}(\Phi,x) \tag{19}$$

(uncorrelated cavitation mechanism is supposed).

The following notations are used for the increments of the work applied, the elastic strain energy and the energy spent for formation of a new surface, S:

$$\mathrm{d}W,\ \ \mathrm{d}U_{\mathrm{e}},\ \ \mathrm{d}U_{\mathrm{S}}, \tag{20}$$

referred to a unit volume of a sample. These increments should be calculated as

$$\mathrm{d}W = \sigma\,\mathrm{d}\varepsilon = \hat{E}(\Phi,x)\varepsilon\,\mathrm{d}\varepsilon, \tag{21a}$$

$$\mathrm{d}U_{\mathrm{e}} = \mathrm{d}\left(\frac{\sigma\varepsilon}{2}\right) = \hat{E}(\Phi,x)\varepsilon\,\mathrm{d}\varepsilon + \frac{\mathrm{d}E(\Phi,x)}{\mathrm{d}x}\,\frac{\varepsilon^2}{2}\mathrm{d}x, \tag{21b}$$

$$\mathrm{d}U_{\mathrm{S}} = 2\gamma\left(\frac{\mathrm{d}S}{\mathrm{d}x}\right)\mathrm{d}x, \tag{21c}$$

under the macroscopic condition of a uniaxial tension.

The energy balance between the terms (20) and (21a)–(21c) is supposed to hold:

$$\mathrm{d}W \geqslant \mathrm{d}U_{\mathrm{e}} + \mathrm{d}U_{\mathrm{S}}, \tag{22a}$$

or, exploring Eqs. (21a)–(21c):

$$0 \geqslant \frac{\mathrm{d}\hat{E}(\Phi,x)}{\mathrm{d}x}\,\frac{\varepsilon^2}{2} + \gamma\frac{\mathrm{d}S}{\mathrm{d}x}. \tag{22b}$$

The strain, ε, and the portion of the cavitated inclusions, x, are linked by the inequality (22a) and (22b), and this coupling is supposed to be monotonously increasing. The last assumption means:

(1) The cavitation of inclusions starts only at $\varepsilon = \varepsilon_{\mathrm{st}}$,

$$\varepsilon_{\mathrm{st}} = \sqrt{-2\gamma\frac{\mathrm{d}S}{\mathrm{d}x}(0)\Big/\frac{\mathrm{d}\hat{E}}{\mathrm{d}x}(\Phi,0)}, \tag{23a}$$

and finishes if $\varepsilon = \varepsilon_{\mathrm{f}}$, where

$$\varepsilon_f = \sqrt{-2\gamma \frac{dS}{dx}(\Phi) \Big/ \frac{d\hat{E}}{dx}(\Phi, \Phi)}. \tag{23b}$$

Outside of the cavitation region, $\varepsilon_{st} \leqslant \varepsilon \leqslant \varepsilon_f$, microfracture events do not occur, $dx = 0$, and the balance (22a) means that the work applied is totally spent for an elastic energy storage:

$$dW = dU_e. \tag{23c}$$

For $\varepsilon \leqslant \varepsilon_{st}$ the uniaxial stress–strain diagram is linear with a slope $E^+(\Phi) = \hat{E}(\Phi, 0)$, correspondent to non-cavitated particles. The portion $\varepsilon_f \leqslant \varepsilon$ of the stress–strain diagram is linear too but with a smaller slope $E^-(\Phi) = \hat{E}(\Phi, \Phi)$, correspondent to a complete transformation of the inclusions into pores.

(2) If at any value of x the expressions (22a) and (22b) form a strong inequality, then, in contrast, the strain increment is supposed to be zero: $d\varepsilon = 0$, and the cavitation of inclusions proceeds at a fixed strain value which reflects in a vertical portion of the stress–strain diagram.

Further, the effective elastic modulus, $\hat{E}(\Phi, x)$, and the new surface, $S(\Phi, x)$, depend on a cavitation mechanism where the equations for these quantities are derived below.

4.1.1. Elastic modulus

The calculation of the elastic modulus, $\hat{E}(\Phi, x)$, and its derivative in a case of an uncorrelated cavitation is performed in two steps using a differential self-consistent approach for each of them. Thereby the pores are considered as inhomogeneities of a concentration x in an effectively homogeneous elastic continuum with the moduli

$$K(\widetilde{\Phi}), \quad \mu(\widetilde{\Phi}) \tag{24}$$

and formed by the matrix and non-crashed inclusions of the concentration

$$\widetilde{\Phi}(\Phi, x) = \frac{\Phi - x}{1 - x}. \tag{25}$$

The following argumentation justifies such a choice of the sequence of steps. Large inclusions cavitate previously to small ones (it will be shown below). So, the consideration of large pores in an effective elastic medium formed by a matrix filled by small inclusions is more natural than an opposite representation.

The effective moduli (24) are equal to those of a matrix if a case of crazing in a homogeneous glassy polymer is analyzed. Eqs. (8a)–(8d) and (11a)–(11c) are used for this purpose in the cases of a particulate filled composite and of a rubber toughened plastic, respectively, with a replacement of Φ by $\widetilde{\Phi}$.

The second step consists of the application of a differential self-consistent approach (10a)–(10d) to the elasticity problem for a porous medium with the associated replacements $\Phi \to x$, $u \to \hat{u}$, $u_m \to u(\widetilde{\Phi})$, $K \to \hat{K}$, $K_m \to K(\widetilde{\Phi})$, $\mu \to \hat{\mu}$ and $\mu_m \to \mu(\widetilde{\Phi})$ for each of the three systems analyzed.

The most simple equation corresponds to a particulate filled composite with a matrix Poisson's ratio of $\nu_m = 0.2$. Using Eqs. (8d) and (10d), one easily obtains:

$$\hat{\nu}(\Phi, x) \equiv \nu_m = 0.2, \quad \hat{E}(\Phi, x) = E_m(1 - x)^4(1 - \Phi)^{-2}. \tag{26}$$

Further, it is sensible to represent here an asymptotic result correspondent to a general case, but for a small concentration limit $\Phi \to 0$. Let us supply every characteristic by superscript "+" and by superscript "−" in the cases of limit cavitation levels: non-cavitated and completely cavitated inclusions, respectively. Particularly,

$$E^+ = \hat{E}(\Phi, 0), \quad \nu^+ = \hat{\nu}(\Phi, 0), \tag{27a}$$

$$E^- = \hat{E}(\Phi, \Phi), \quad \nu^- = \hat{\nu}(\Phi, \Phi). \tag{27b}$$

In the small concentration limit it is sufficient to use a linear approximation for the elastic characteristics of a composite with respect to the filler volume fraction. Accepting this simplification it follows:

$$E^{+}(\Phi) \approx E_{\mathrm{m}}\left(1+\alpha_{\mathrm{m}}^{+}\Phi\right), \tag{28a}$$

$$E^{-}(\Phi) \approx E_{\mathrm{m}}\left(1-\alpha_{\mathrm{m}}^{-}\Phi\right) \tag{28b}$$

with

$$E_{\mathrm{m}}\alpha_{\mathrm{m}}^{+} = \left.\frac{\mathrm{d}E^{+}(\Phi)}{\mathrm{d}\Phi}\right|_{\Phi=0}, \quad E_{\mathrm{m}}\alpha_{\mathrm{m}}^{-} = -\left.\frac{\mathrm{d}E^{-}(\Phi)}{\mathrm{d}\Phi}\right|_{\Phi=0}.$$

By using the notation (25) one gets:

$$\hat{E}(\Phi,x) \approx E(\widetilde{\Phi})(1-\alpha^{-}(\widetilde{\Phi})x) \approx E_{\mathrm{m}}\left(1+\alpha_{\mathrm{m}}^{+}\left(\frac{\Phi-x}{1-x}\right)\right)\left(1-\alpha_{\mathrm{m}}^{-}x\right) \tag{29}$$

and in the limit $x \to 0$, $\Phi \to 0$:

$$\left.\frac{\mathrm{d}\hat{E}(\Phi,x)}{\mathrm{d}x}\right|_{x\to 0,\Phi\to 0} = -E_{\mathrm{m}}\left(\alpha_{\mathrm{m}}^{+}+\alpha_{\mathrm{m}}^{-}\right). \tag{30}$$

Referring to an analysis of a general version of the correlated mechanism (Fig. 4c, arbitrary slope φ), a particular case of a transverse zone (Fig. 3b, $\varphi = 0$) should be previously treated. It is convenient to perform calculations in terms of a compliance tensor, J_{ijkl}. The analysis is reduced to a calculation of a compliance tensor $\hat{J}^{\mathrm{c}}_{ijkl}(\varphi)$ correspondent to a laminated composite consisting of two layers of compliances J^{+}_{ijkl} and J^{-}_{ijkl}. These layers are isotropic and the tensors J^{+}_{ijkl} and J^{-}_{ijkl} are determined by a couple of elastic constants, $E^{+(-)}$, $v^{+(-)}$, for instance:

$$J^{+(-)}_{iiii} = \frac{1}{E^{+(-)}}, \quad J^{+(-)}_{iijj} = -\frac{v^{+(-)}}{E^{+(-)}}, \quad J^{+(-)}_{ijij} = \frac{1+v^{+(-)}}{2E^{+(-)}}, \qquad i \neq j. \tag{31}$$

By introducing the quantity a, $0 \leqslant a \leqslant 1$, as a relative portion of a porous region,

$$a = \frac{x}{\Phi}, \tag{32}$$

accepting x_1 as a stretching axis as well as by using the well-known elasticity theory for a laminated composite a transversely symmetric compliance tensor $\hat{J}^{\mathrm{c}}_{ijkl}(0)$ can be described as follows:

$$\hat{J}^{\mathrm{c}}_{1111}(0) = J^{+}_{1111}(1-a) + J^{-}_{1111}a - \frac{2\left(J^{+}_{1122}-J^{-}_{1122}\right)^{2}a(1-a)}{(J^{+}_{1111}+J^{+}_{1122})a + (J^{-}_{1111}+J^{-}_{1122})(1-a)}, \tag{33a}$$

$$\hat{J}^{\mathrm{c}}_{1122}(0) = \hat{J}^{\mathrm{c}}_{1133}(0) = \frac{J^{+}_{1122}\left(J^{-}_{1111}+J^{-}_{1122}\right)(1-a) + J^{-}_{1122}(J^{+}_{1111}+J^{+}_{1122})a}{(J^{+}_{1111}+J^{+}_{1122})a + (J^{-}_{1111}+J^{-}_{1122})(1-a)}, \tag{33b}$$

$$\hat{J}^{\mathrm{c}}_{2222}(0) = \hat{J}^{\mathrm{c}}_{3333}(0) = \frac{\alpha\left(J^{+}_{1111}a + J^{-}_{1111}(1-a)\right) - \beta\left(J^{+}_{1122}a + J^{-}_{1122}(1-a)\right)}{\left(J^{+}_{1111}a + J^{-}_{1111}(1-a)\right)^{2} - \left(J^{+}_{1122}a + J^{-}_{1122}(1-a)\right)^{2}}, \tag{33c}$$

$$\hat{J}^{\mathrm{c}}_{1212}(0) = \hat{J}^{\mathrm{c}}_{1313}(0) = aJ^{-}_{1212} + (1-a)J^{+}_{1212} \tag{33d}$$

with

$$\alpha = J^{+}_{1111}J^{-}_{1111} + J^{+}_{1122}J^{-}_{1122},$$

$$\beta = J^{+}_{1111}J^{-}_{1122} + J^{-}_{1111}J^{+}_{1122}.$$

Let us now turn to an arbitrary slope, φ, of a microporous zone (Fig. 3c). By applying a general tensor transformation law

$$\hat{J}^{c}_{ijkl}(\varphi) = a_{im}a_{jn}a_{kp}a_{lq}\hat{J}^{c}_{mnpq}(0) \tag{34a}$$

with

$$\|a_{ij}(\varphi)\| = \begin{pmatrix} \cos\varphi & -\sin\varphi & 0 \\ \sin\varphi & \cos\varphi & 0 \\ 0 & 0 & 1 \end{pmatrix},$$

it follows:

$$\hat{J}^{c}_{1111}(\varphi) = \frac{1}{4}\cos^2 2\varphi(\hat{J}^{c}_{1111}(0) + \hat{J}^{c}_{2222}(0) - 2\hat{J}^{c}_{1122}(0) - 4\hat{J}^{c}_{1212}(0)) + \frac{1}{2}\cos 2\varphi(J^{c}_{1111}(0) - J^{c}_{2222}(0)) + \frac{1}{4}(\hat{J}^{c}_{1111}(0) + \hat{J}^{c}_{2222}(0) + 2\hat{J}^{c}_{1122}(0) + 4\hat{J}^{c}_{1212}(0)). \tag{34b}$$

A similar equation holds true for the x-derivative, $\left(\hat{J}^{c}_{1111}(\varphi)\right)_x$. In the case of transverse zones corresponding derivatives can be calculated by using Eqs. (32) and (33a)–(33d):

$$(\hat{J}^{c}_{ijkl}(0))_x = \frac{(\hat{J}^{c}_{ijkl}(0))_a}{\Phi}. \tag{35}$$

Similarly to the case of an uncorrelated cavitation, it is also worthwhile to determine the data correspondent to the limit $x \to 0$, $\Phi \to 0$. One gets:

$$(\hat{J}^{c}_{1111}(0))_x\Big|_{x\to 0,\Phi\to 0} = \frac{J^{-}_{1111} - J^{+}_{1111}}{\Phi}, \tag{36a}$$

$$(\hat{J}^{c}_{1122}(0))_x\Big|_{x\to 0,\Phi\to 0} = \frac{J^{-}_{1122} - J^{+}_{1122}}{\Phi}, \tag{36b}$$

$$(\hat{J}^{c}_{2222}(0))_x\Big|_{x\to 0,\Phi\to 0} = \frac{J^{-}_{2222} - J^{+}_{2222}}{\Phi}, \tag{36c}$$

$$(\hat{J}^{c}_{1212}(0))_x\Big|_{x\to 0,\Phi\to 0} = \frac{J^{-}_{1212} - J^{+}_{1212}}{\Phi}. \tag{36d}$$

Further, a substitution of Eqs. (33a)–(33d) into Eq. (34b) and of Eqs. (36a)–(36d) into the equation for the x-derivatives obviously gives

$$\hat{J}^{c}_{1111}(\varphi)|_{x\to 0,\Phi\to 0} \equiv \hat{J}^{c}_{1111}(0)|_{x\to 0,\Phi\to 0} = \frac{1}{E_m}, \tag{37a}$$

$$(\hat{J}^{c}_{1111}(\varphi))_x|_{x\to 0,\Phi\to 0} \equiv (\hat{J}^{c}_{1111}(0))_x|_{x\to 0,\Phi\to 0} = \frac{J^{-}_{1111} - J^{+}_{1111}}{\Phi} = \frac{\alpha^{-}_m + \alpha^{+}_m}{E_m} \tag{37b}$$

and for $\left(\hat{E}_c\right)_x = d\hat{E}_c/dx$:

$$(\hat{E}_c)_x|_{x\to 0,\Phi\to 0} = \frac{1}{(\hat{J}^{c}_{1111})_x}\Bigg|_{x\to 0,\Phi\to 0} = -\frac{(\hat{J}^{c}_{1111})_x}{(\hat{J}^{c}_{1111})^2}\Bigg|_{x\to 0,\Phi\to 0} = -E_m(\alpha^{-}_m + \alpha^{+}_m). \tag{37c}$$

It is important to note that one obtains a rigorous proof of the following statement. Both the stiffness and the stiffness derivative with respect to a cavitated portion, x, of inclusions do not depend upon whether an uncorrelated or a correlated cavitation exists in the small concentration limit. This conclusion seems to be intuitively true because a correlation in the proceeding of any events will not be important if the number of events tends to zero.

4.1.2. Surface area

In the following section the uncorrelated and the correlated cavitation mechanisms will also be analyzed. Let $p(r)$ be a particle size distribution, i.e. $p(r)\mathrm{d}r$ defines a volume portion of particles with the radii in the interval $r \div r + \mathrm{d}r$. The ordered particle size sequence which is a case of a spatial uncorrelated cavitation suggests for every given x a complete crash of a particle at any point of the volume in the interval $r_1(x) \leqslant r \leqslant r_2(x)$. Obviously $r_1(x)$ and $r_2(x)$ are decreasing and increasing functions, respectively. x, r_1, r_2 and S are related to each other as follows:

$$x = \Phi \frac{\int_{r_1(x)}^{r_2(x)} p(r)\mathrm{d}r}{\int_0^\infty p(r)\mathrm{d}r}, \quad S(x) = \Phi \frac{\int_{r_1(x)}^{r_2(x)} p(r)\frac{4\pi r^2}{(4/3)\pi r^3}\mathrm{d}r}{\int_0^\infty p(r)\mathrm{d}r} = \Phi \frac{\int_{r_1(x)}^{r_2(x)} \frac{3p(r)}{r}\mathrm{d}r}{\int_0^\infty p(r)\mathrm{d}r}. \tag{38}$$

Thus, the relation holds true:

$$\frac{\mathrm{d}S}{\mathrm{d}x} = \frac{3}{r_1(x)} + \frac{3}{r_2(x)} \tag{39a}$$

and it becomes clear, that the larger $r_1(x)$ and $r_2(x)$ are, the smaller is the derivative $\mathrm{d}S/\mathrm{d}x$ and the more advantageous is a cavitation. Therefore, a decreasing size order is the most advantageous for a cavitation. Particularly, r_2 should be infinite and after a re-denotation $r_1(x) \to r(x)$ Eq. (39a) transforms into:

$$\frac{\mathrm{d}S}{\mathrm{d}x} = \frac{3}{r(x)}. \tag{39b}$$

A correlated cavitation mechanism supposes a correlation in a spatial position of pores formed but a simultaneous cavitation of inclusions in corresponding zones independently of their size. Such an assumption leads to an independence of the derivative:

$$\frac{\mathrm{d}S}{\mathrm{d}x} = \mathrm{const} = 3\frac{\int_0^\infty \frac{p(r)}{r}\mathrm{d}r}{\int_0^\infty p(r)\mathrm{d}r}. \tag{39c}$$

If a particle size distribution is a narrow one, then the Eqs. (39b) and (39c) predict the same values.

Nevertheless, a general case of an arbitrary particle size distribution can be analyzed. A smooth distribution formed by second order splines is chosen for the analysis:

$$p(r) = 2\left(\frac{r - r_{\min}}{\Delta_\mathrm{l}}\right)^2 \quad \text{for } r_{\min} \leqslant r \leqslant r_\mathrm{l}, \tag{40a}$$

$$p(r) = 1 - 2\left(\frac{r - r_{\mathrm{ml}}}{\Delta_\mathrm{l}}\right)^2 \quad \text{for } r_\mathrm{l} \leqslant r \leqslant r_{\mathrm{ml}}, \tag{40b}$$

$$p(r) = 1 \quad \text{for } r_{\mathrm{ml}} \leqslant r \leqslant r_{\mathrm{mr}}, \tag{40c}$$

$$p(r) = 1 - 2\left(\frac{r - r_{\mathrm{mr}}}{\Delta_\mathrm{r}}\right)^2 \quad \text{for } r_{\mathrm{mr}} \leqslant r \leqslant r_\mathrm{r}, \tag{40d}$$

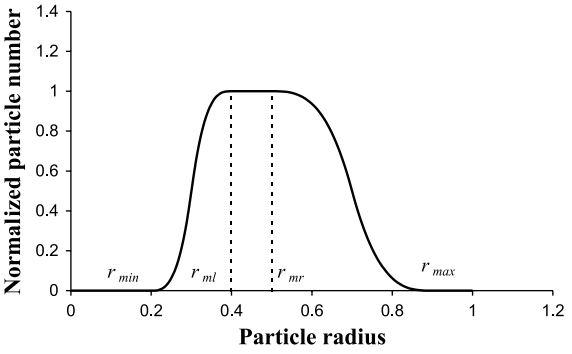

Fig. 5. Sketch of a particle size distribution.

$$p(r) = 2\left(\frac{r - r_{\max}}{\Delta_{\mathrm{r}}}\right)^2 \quad \text{for } r_{\mathrm{r}} \leqslant r \leqslant r_{\max}, \tag{40e}$$

$$p(r) = 0 \quad \text{otherwise.} \tag{40f}$$

A shape of the distribution (40a)–(40f) is depicted in Fig. 5 and the parameters introduced are linked by the relations:

$$\Delta_{\mathrm{l}} = r_{\mathrm{ml}} - r_{\min}, \quad r_{\mathrm{l}} = \frac{r_{\mathrm{ml}} + r_{\min}}{2}, \quad \Delta_{\mathrm{r}} = r_{\max} - r_{\mathrm{mr}}, \quad r_{\mathrm{r}} = \frac{r_{\mathrm{mr}} + r_{\max}}{2}.$$

In the following a symmetric particular case of Eqs. (40a)–(40f)

$$r_{\min} = R - (k+1)\Delta, \quad r_{\mathrm{ml}} = R - k\Delta, \quad r_{\mathrm{mr}} = R + k\Delta, \quad r_{\max} = R + (k+1)\Delta \tag{41}$$

is considered. The parameter k determines the sharpness of the distribution. R is equal to a mean radius

$$R = \bar{r} = \frac{M_1}{M_0}, \tag{42}$$

and the dispersion $d = \sqrt{\overline{r^2} - \bar{r}^2}$ is determined by the formula:

$$d = \Delta\sqrt{\frac{16k^3 + 24k^2 + 14k + 3}{24(2k+1)}}, \tag{43}$$

M_n is a widely accepted denotation for a distribution moment:

$$M_n = \int_0^\infty r^n p(n)\,\mathrm{d}n. \tag{44}$$

The same values of $\bar{r}$ and d can be obtained for various Δ and k values. The variation of these parameters at fixed values of $\bar{r}$ and d will be classified in a further analysis as an effect of the distribution shape.

4.2. Deformation diagrams

Cavitation kinetics and corresponding stress–strain diagrams of particulate composites, rubber toughened plastics and glassy polymers under a uniaxial tension are represented in Figs. 6–8, respectively.

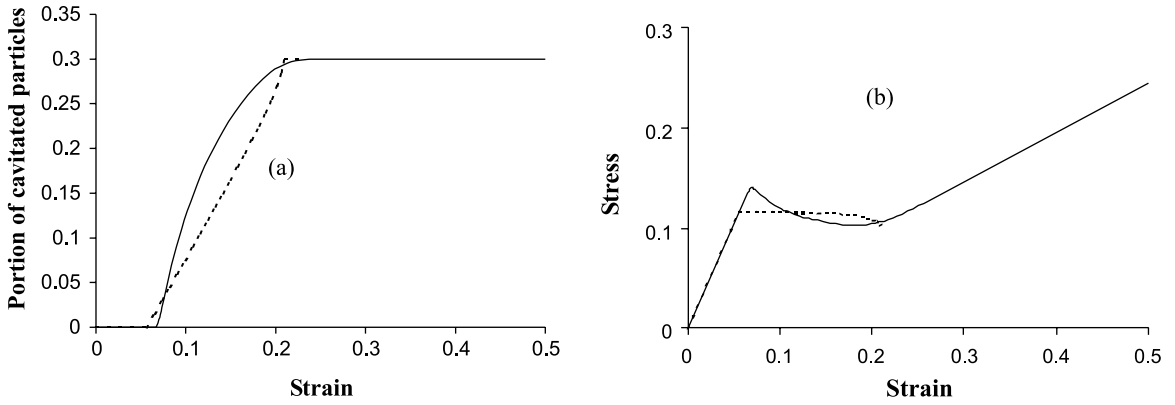

Fig. 6. Kinetics of debonding and corresponding non-linear stress–strain uniaxial diagrams for a particulate filled composite, calculated in the frameworks of an uncorrelated (—) and a correlated (···) mechanism at $\Phi = 30$ vol.%. Matrix characteristics: $E_m = 1$, $\nu_m = 0.3$; reduced specific surface energy: $\bar{\gamma} = 0.0004$; parameters of particle size distribution: $\bar{r} = 1$; $d = 0.3$; $k = 1$.

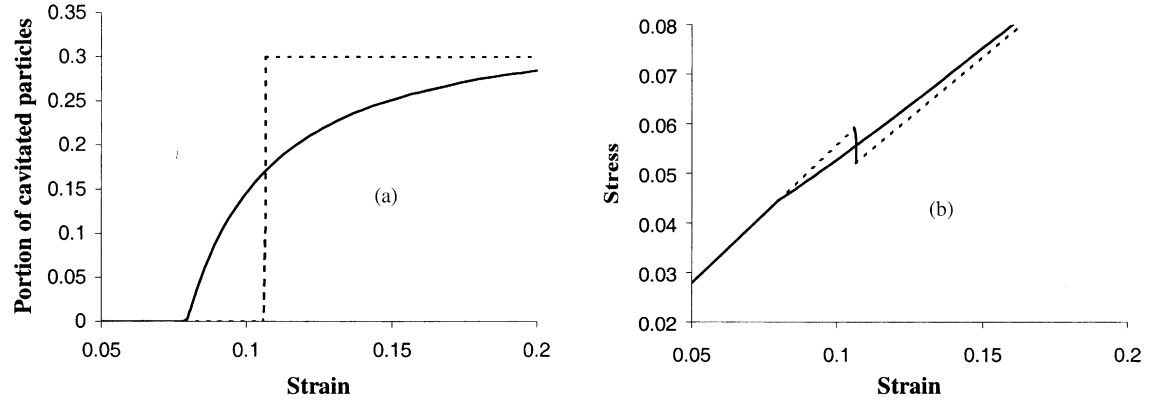

Fig. 7. Kinetics of elastomeric inclusions failure and corresponding non-linear stress–strain uniaxial diagrams for a rubber toughened plastic, calculated in the frameworks of an uncorrelated (—) and a correlated (···) mechanism at $\Phi = 30$ vol.%. Matrix characteristics: $E_m = 1$, $\nu_m = 0.3$; rubbery inclusion shear modulus: 0.01; reduced specific surface energy: $\bar{\gamma} = 0.0004$; parameters of particle size distribution: $\bar{r} = 1$; $d = 0.3$; $k = 5$.

The following common and distinguished features are seen:

1. The accumulation of pores is accompanied by a drop in the secant elastic modulus for every system and cavitation mechanism. Naturally, the gap between the maximum (no cavitated inclusion) and minimum (every inclusion is cavitated) of a modulus is widest for the case of a particulate filled composite (Fig. 6b) and narrowest for the case of a rubber toughened plastic (Fig. 7b). Nevertheless, that both the matrix and the inclusions are supposed to be elastic, the diagrams are non-linear and even exhibit a maximum for an uncorrelated mechanism of debonding, Fig. 6b, or a correlated mechanism of elastomeric inclusions failure, Fig. 7b, for example.
2. Cavitation mostly proceeds in a non-sharp manner with a gradual accumulation of the pores. An exclusion exists in the case of correlated elastomeric inclusions (dotted lines in Fig. 7). That means a failure of all the particles occurs simultaneously or almost simultaneously.

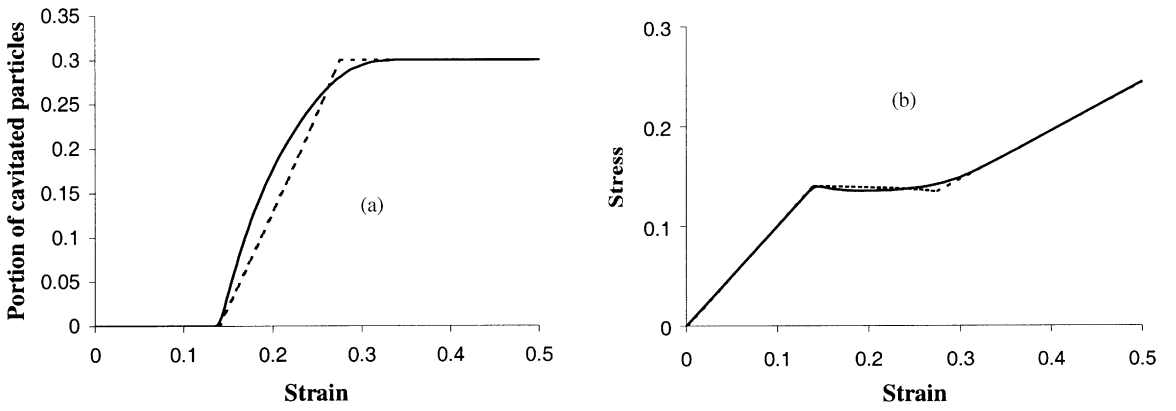

Fig. 8. Kinetics of delocalized (—) and localized (···) crazing and corresponding non-linear stress–strain uniaxial diagrams for a glassy polymer calculated at $\Phi = 30$ vol.% of modeling defects capable for a cavitation. Matrix characteristics: $E_m = 1$, $\nu_m = 0.3$; reduced specific surface energy: $\bar{\gamma} = 0.01$; parameters of particle size distribution: $\bar{r} = 1$; $d = 0.3$; $k = 1$.

3. The model predicts that a minimum strain value, ε_{st}, associated to a start of a cavitation corresponds to an uncorrelated or a correlated mechanism which depends upon the special system. For example, for 30 vol.% of a filler fraction and the same parameters of a particle size distribution (Figs. 6–8) the debonding mechanism primary starts in a particulate filled composite; the uncorrelated failure of elastomeric particles occurs previously to a correlated one in a rubber toughened plastic; delocalized and localized crazing in a glassy polymer start almost at the same strain value. A relationship between these two characteristic strain values is very important and will be discussed below.

4.3. The slope of microporous zones

The technique developed (Eqs. (33a)–(34b)) gives the possibility not only to describe the deformation accompanied by a correlated formation of the pores in arbitrary sloped zones, but also to minimize the strain correspondent to a start of a cavitation by a proper choice of the angle of the zones disposition.

The model predicts a transverse disposition of microporous zones formed by the way of an elastomeric inclusions failure with respect to the tension direction. It makes sense to remind that the ratio of the shear modulus of an inclusion to those of the matrix was chosen as $\mu_i/\mu_m = 10^{-2}$. The slope of the zones formed by debonding (Fig. 9a, filled circled) and by crazing (Fig. 9a, open circles) is about 30° and drops slightly with the fraction of inhomogeneities.

Moreover, it is suitable to note here that the conclusion concerning zero slope in the case of elastomeric inclusions failure contradicts with the results of Lazzery and Bucknall (1995). Firstly, they found experimentally by a microscopic observation that the slope is about 11°, and secondly, they delivered a theoretical estimation describing this value with a good accuracy. However, the contradiction disappears if one keeps in mind that Lazzery's and Bucknall's estimate was derived for the slope of shear bands in a dilatation sensitive plastic medium. Therefore, it is supposed that pores were formed previously or at least during a plastic flow whenever the prediction of our model corresponds to a cavitation in an elastic stage of deformation.

Thus, the model predicts the transverse disposition of microporous zones formed by a cavitation of very soft inclusions ($\mu_i/\mu_m = 10^{-2}$) and a slope of the last if the inclusions are sufficiently stiff ($\mu_i/\mu_m = 1$). The results of a detailed analysis of the slope dependence on the ratio of the inclusion to matrix modulus are represented in Fig. 9b for an inclusion volume fraction $\Phi = 0.1$ (circles); 0.3 (triangles); 0.5 (squares). A

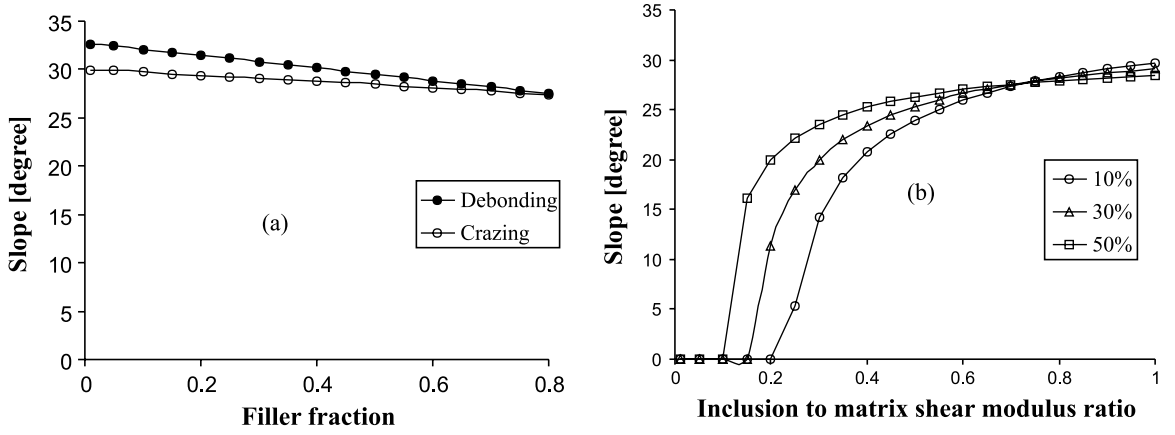

Fig. 9. Slopes of craze-like zones with respect to the direction of tension. Plots are drawn versus filler fraction (a) and inclusion to matrix shear modulus ratio (b). Filled circles (a) correspond to the debonding mechanism of the cavitation, (○) (a) correspond to a crazing in a glassy polymer. A cavitation mechanism of an inclusion rupture is analyzed in figure (b) at 10% (●); 30% (△); 50% (□) of a filler fraction.

rather sharp transition from perpendicular to sloped microporous zones occurs with an increase in the inclusion stiffness at $\mu_i/\mu_m = 0.1$–0.3, and the corresponding angle is about 25–30°.

4.4. Uncorrelated–correlated transition

The principle of the minimum work of deformation has been chosen as a criterion for the existence of an uncorrelated or a correlated cavitation. As it was already discussed, initial linear portions of the diagrams (Figs. 6–8b) correspond to the absence of pores and, hence, do not depend on a mechanism of cavitation. The accumulation of pores causes a decrease of the secant modulus and thereby of the work of deformation. Thus, the principle of minimum work is equivalent to the principle of the start of a cavitation.

Summarizing the arguments given, we can define a ratio of a strain correspondent to a start of an uncorrelated cavitation, ε_{st}^{u}, to a strain correspondent to a start of a correlated cavitation, ε_{st}^{c}, as a value responsible for the proceeding of an uncorrelated or a correlated mechanism, respectively. If $\varepsilon_{st}^{u}/\varepsilon_{st}^{c} < 1$, then an uncorrelated mechanism governs by cavitation. If $\varepsilon_{st}^{u}/\varepsilon_{st}^{c} > 1$, then a formation of crazes or craze-like zones is more advantageous than a diffuse cavitation. A condition $\varepsilon_{st}^{u}/\varepsilon_{st}^{c} = 1$ serves as a criterion for a transition from an uncorrelated to a correlated cavitation.

The results of a simulation for the existence of a diffuse or a correlated cavitation by debonding, elastomeric inclusion failure and on defects in homogeneous polymers are represented in Figs. 10–12, respectively. It is worthwhile to underline the following regularities found:

1. The cavitation laws are very similar for every system studied.
2. The previous analysis has shown that correspondent to the values of the elastic modulus (compare Eqs. (30) and (37c)) and the surface area (compare Eqs. (39b) and (39c) for a narrow particle size distribution), the strain values ε_{st}^{u} and ε_{st}^{c} are equal in the limit $\Phi \to 0$, $d \to 0$.
3. An increase in the inhomogeneities fraction naturally causes a mutual influence of the pores and a tendency to a cooperation which becomes reflected in an increase in the ratio $\varepsilon_{st}^{u}/\varepsilon_{st}^{c}$.
4. An increase in the width of a particle size distribution (dispersion d) at a fixed mean size of the particles noticeably reduces the surface area derivative (see Eqs. (22a) and (22b)) at the start of a cavitation in the case of an uncorrelated mechanism because large inclusions can be crashed first. On the contrary the

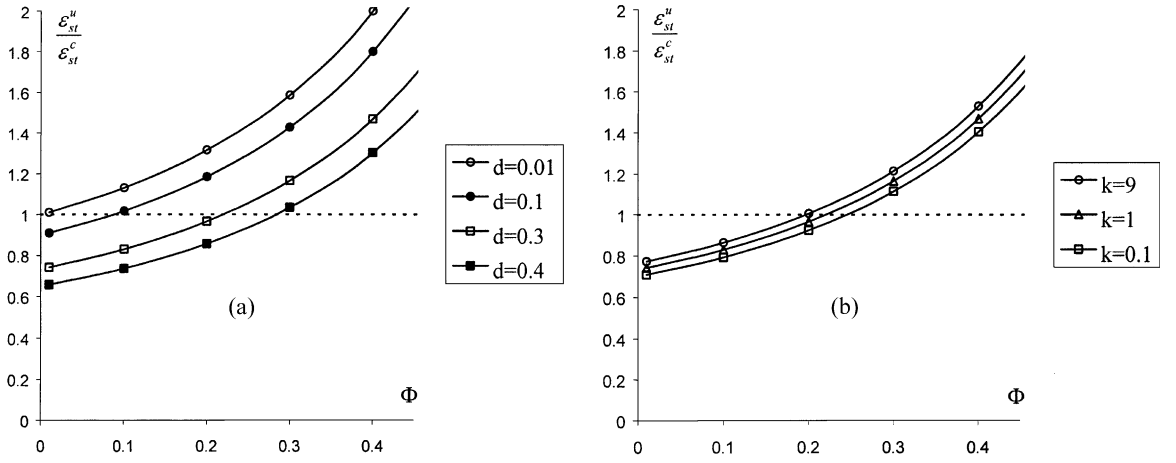

Fig. 10. Ratio of a strain, ε^{u}_{st}, correspondent to a start of an uncorrelated debonding to that correspondent to a correlated mechanism, ε^{c}_{st}, versus a rigid particle fraction, Φ, at various width, d, but of a fixed shape, $k = 1$, (a), as well as at a various shape of a particle size distribution but at a fixed width, $d = 0.3$ (b).

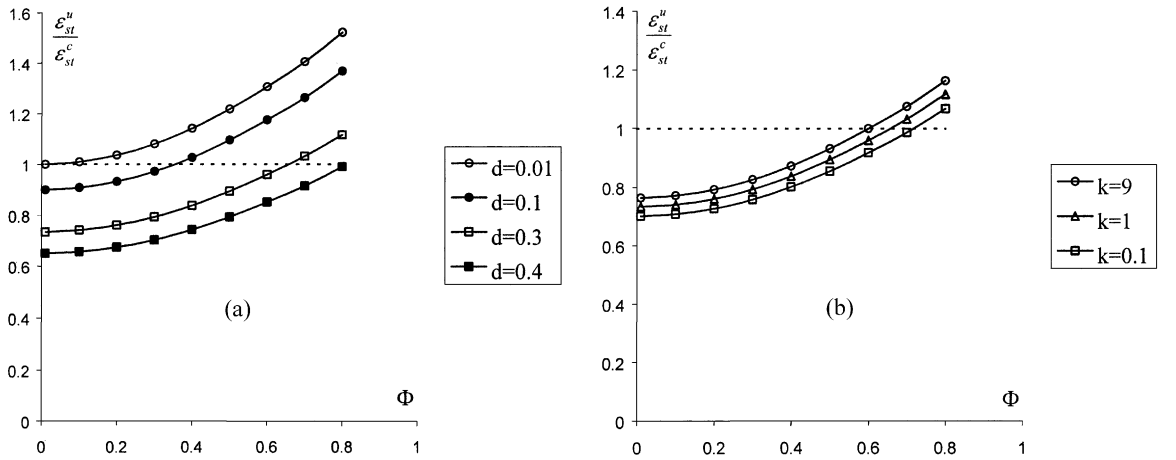

Fig. 11. Ratio of a strain, ε^{u}_{st}, correspondent to a start of an uncorrelated elastomeric inclusions failure to that of a correlated mechanism, ε^{c}_{st}, versus the inclusion fraction, Φ, at various width, d, but of a fixed shape, $k = 1$, (a), and at a various shape of an inclusions size distribution but at a fixed width, $d = 0.3$ (b).

mean size is responsible for the corresponding constant value of this derivative in case of a correlated mechanism (see Eq. (39c)). Thereby an increase in d causes the decrease in the ratio $\varepsilon^{u}_{st}/\varepsilon^{c}_{st}$, particularly, the transitional point $\varepsilon^{u}_{st}/\varepsilon^{c}_{st} = 1$ has been shifted to a larger filler fraction Φ.

5. A decrease in the k-value means a change in the shape of a particle size distribution from a sharp to a gradual vanishing (see Fig. 5 and Eqs. (40a)–(40f) and (41)). A large k-value means an extended plateau in comparison with a transitional portion. On the contrary, the limit $k \to 0$ means an absence of the plateau. Furthermore, it can be stated that a more gradual distribution at a fixed width (Figs. 10–12b) provides smaller values of the strain ratio $\varepsilon^{u}_{st}/\varepsilon^{c}_{st}$, and hence, an increase in the critical inhomogeneities fraction. However, the effect is not greatly emphasized.

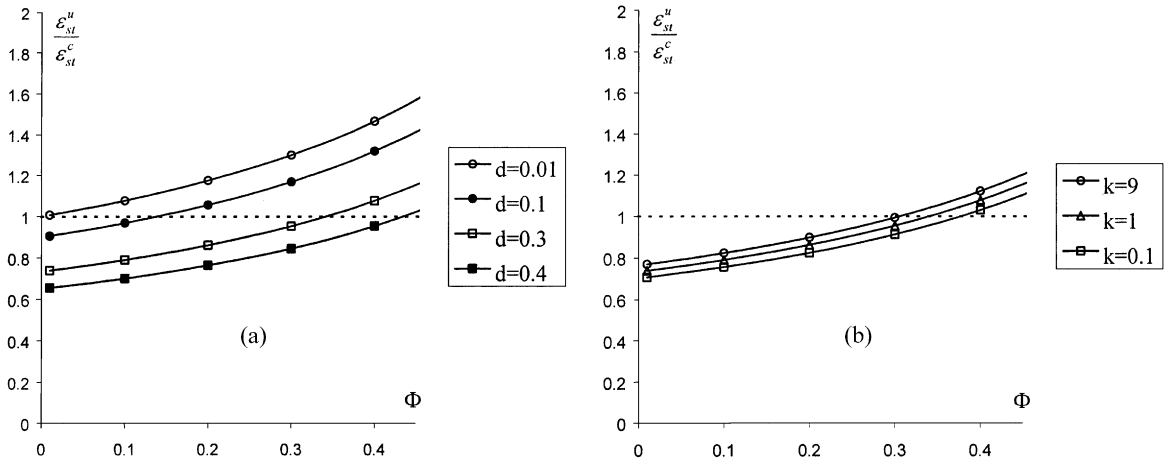

Fig. 12. Ratio of a strain, ε^{u}_{st}, correspondent to a start of delocalized crazing to that correspondent to a localized one, ε^{c}_{st}, versus the defect volume fraction, Φ, at various width, d, but of a fixed shape, $k = 1$ (a), and at a various shape of a defect size distribution but at a fixed width, $d = 0.3$ (b).

6. The most sharp $\varepsilon^{u}_{st}/\varepsilon^{c}_{st}$ concentration dependence corresponds to the debonding mechanism of a cavitation in particulate filled composites which provides smaller values for the critical fractions. The significance of this law consists in a most essential change of the material stiffness as a result of a replacement of rigid inclusions by pores.

5. Conclusion

1. A comparable analysis of the laws of pores formation in three systems—particulate filled composites, rubber toughened polymers and individual polymer solids—has been performed in the framework of a general model proposed.
2. Two sides of the problem have been considered. Conditions and completeness of an individual cavitation is the first. Correlation of microfracture events on neighboring inclusions and the position of microporous zoned is the second.
3. A number of important common features of an individual cavitation has been established. Namely, the link between the stress sufficient for a cavitation and the size of the defect responsible for the formation of a pore was found. Particularly, the critical stress value below which a defect of any size is disable for the transformation into a pore was estimated. Above this critical value a range of the defects, sizes exists which are effective as sources of pores: the higher the stress is, the wider is the range.
4. The most important difference in the laws of an individual cavitation for the three systems studied is their completeness: the stiffer the inclusion is, the closer is the size of the pore to the size of the inclusion from which the pore is formed.
5. The model developed predicts an uncorrelated cavitation at a low inclusions fraction and a correlation of microfracture events on neighboring particles at their high content. Thus, an increase in inclusion's fraction causes an uncorrelated–correlated transition. The wider the particle size distribution is, and the softer the inclusions are, the larger is the transitional fraction value.
6. If a correlated cavitation occurs, then the inclusion stiffness affects the slope of the microporous zones to a plane transverse to the tension axis. There exists a threshold value of 0.1–0.3 for the shear modulus

ratio, μ_i/μ_m (the threshold value is dependent on the inclusion fraction), below which craze-like zones should be transverse to the tension axis. Such a situation exists in case of the failure of elastomeric inclusions failure. The model predicts a sharp increase in the slope upto approximately 30° above the critical value of the relative inclusion stiffness.

Acknowledgements

V. Oshmyan would like to thank the Russian Foundation of Basic Research, grant no. 00-03-33169, and the German Research Foundation for a grant (Mercator guest professorship) as well as the Laboratory for Technical Mechanics (Head: Prof. Dr. K. Herrmann) at Paderborn University for the excellent working conditions.

References

Anderson, L.L., Farris, R.J., 1988. A predictive model to the mechanical behavior of particulate composites. Polym. Eng. Sci. 28, 522–528.

Bazhenov, S., 1995. Effect of particles on failure modes of filled polymers. Polym. Eng. Sci. 35, 813–822.

Berlin, A.A., Wolfson, S.A., Oshmyan, V.G., Enikolopyan, N.S., 1990. Principles for Polymer Composites Projection. Khimiya, Moscow.

Berlin, A.A., Zhuk, A.V., Knunyantz, N.N., Oshmyan, V.G., Topolkaraev, V.A., 1991. Regularities of adhesive failure in particulate filled polymers. Macromol. Chem. Macromol. Sym. 44, 295–302.

Berlin, A.A., Knunyantz, N.N., Oshmyan, V.G., Timan, S.A., Zhuk, A.V., Topolkaraev, V.A., 1992. Mathematical simulation of adhesive failure in particle filled composites and its effect on the strength of materials. In: Mileiko, S.T., Tvardovski, V.V. (Eds.), International Symposium on Composites: Fracture Mechanics and Technology, Chernogolovka, Russia, 1992, pp. 114–125.

Bucknall, C.B., 1977. Toughened Plastics. Applied Science Publishers, London.

Christensen, R.M., 1979. Mechanics of Composite Materials. Wiley, New York.

D'Orasio, L., Mansarella, C., Martuscelli, E., Polato, F., 1991. Polypropylene/ethylene-co-propylene blends: influence of molecular structure and composition of EPR on melt reology, morphology and impact properties of injection-molded samples. Polymer 32, 1186–1194.

Dekkers, H.E.J., Heikens, D., 1986. Interfacial effects on local deformation mechanism in glass bead filled glassy polymers. In: Ishida, H., Koening, J.L. (Eds.), Composite Interfaces. Elsevier Science Publ. Co. Inc., New York, pp. 161–169.

Dubnikova, I.L., Oshmyan, V.G., 1998. The effect of inclusion size on the interfacial debonding process and yield stress of highly filled plastic polymers. Polym. Sci. 40, 925–933.

Dubnikova, I.L., Gorenberg, A.Ya., Oshmyan, V.G., 1997a. Mechanisms of particulate filled polypropylene: finite plastic deformation and fracture. J. Mater. Sci. 32, 1613–1622.

Dubnikova, I.L., Muravin, D.K., Oshmyan, V.G., 1997b. Debonding and fracture of particulate filled isotactic polypropylene. Polym. Eng. Sci. 37, 1301–1313.

Fu, Q., Wang, G., 1993. Effect of morphology on brittle–ductile transition of HDPE/$CaCO_3$ blends. J. Appl. Polym. Sci. 49, 1985–1988.

Fu, Q., Wang, G., Shen, J., 1993. Polyethylene toughened by $CaCO_3$ particles: brittle–ductile transition of $CaCO_3$ toughened HDPE. J. Appl. Polym. Sci. 49, 23–28.

Gent, A.N., 1984. Failure processes in elastomers at or near a rigid spherical inclusion. J. Mater. Sci. 19, 1947–1956.

Gorbunova, N.V., Knunyantz, N.N., Manevitch, L.I., Oshmyan, V.G., Topolkaraev, V.A., 1990. Effect of interfacial bond strength on the elastic–plastic properties of particulate filled composite material. Mech. Compos. Mater. 2, 336–339.

Hashin, Z., 1962. The elastic moduli of heterogeneous materials. J. Appl. Mech. 29, 143–165.

Herrmann, K.P., Oshmyan, V.G., 1997. Regularities of fracture of elastomeric inclusions in a particulate filled brittle matrix composite. In: Brandt, A.M., Li, V.C., Marshall, I.H. (Eds.), Proceedings of the International Symposium on Brittle Matrix Composites 5, Warsaw, Poland, 1997. BIGRAF and Woodhead Publ., Warsaw, pp. 399–408.

Inoue, T., Suzuki, T., 1994. Selective crosslinking reaction in polymer blends. II. Its effect on impact strength and other mechanical properties of polypropylene/unsaturates elastomer blends. J. Appl. Polym. Sci. 54, 723–733.

Inoue, T., Suzuki, T., 1995. Selective crosslinking reaction in polymer blends. III. The effects of the crosslinking of dispersed EPDM particles on the impact behavior of PP/RPDM blends. J. Appl. Polym. Sci. 56, 1113–1125.

Ishikawa, M., 1995. Stability of plastic deformation and toughness of polycarbonate blended with poly(acrylonitrile–butadiene–styrene) co-polymer. Polymer 36, 2203–2210.

Ishikawa, M., Chiba, I., 1990. Toughening mechanism of blends of poly(acrylonitrile–butadiene–styrene) co-polymer and BPA polycarbonate. Polymer 31, 1232–1238.

Ishikawa, M., Sugimoto, M., Inoue, T., 1996. Mechanism of toughening for polypropylene blended with ethylene–propylene–diene rubber following selective crosslinking. J. Appl. Polym. Sci. 62, 1495–1502.

Kikuchi, Y., Fukui, T., Okada, T., Inoue, T., 1991. Elastic–plastic analysis of the deformation mechanism of PP-EPDM thermoplastic elastomer: origin of rubber elasticity. Polym. Eng. Sci. 31, 1029–1032.

Kikuchi, Y., Fukui, T., Okada, T., Inoue, T., 1992. Origin of rubber elasticity in thermoplastic elastomers consisting of crosslinked rubber particles and ductile matrix. J. Appl. Polym. Sci.: Appl. Polym. Symp. 50, 261–271.

Kim, G.-M., Michler, G.H., Gahleitner, M., Fiebig, J., 1996. Relationship between morphology and micromechanical toughening mechanisms in modified polypropylenes. J. Appl. Polym. Sci. 60, 1391–1403.

Knunyantz, N.N., Oshmyan, V.G., 1992. Simulation of adhesive failure regularities in particulate filled composites in the frameworks of composite sphere and periodic structural model.

Knunyantz, N.N., Manevitch, L.I., Oshmyan, V.G., Tovmasyan, Yu.M., Topolkaraev, V.A., 1983. On the effect of adhesion on elastic properties of particulate filled composite. Dokladi Akademii Nauk SSSR 270, 803–806.

Knunyantz, N.N., Lyapunova, M.A., Manevitch, L.I., Oshmyan, V.G., Shaulov, A.Yu., 1986. Simulation of the influence of a non-ideal adhesive bond on the elastic properties of particulate filled composites. Mech. Compos. Mater. 2, 231–234.

Kozii, V.V., Rosenberg, B.A., 1992. Mechanisms of an energy dissipation in thermoset polymers, filled by an elastomer. Polym. Sci. (A) 34, 3–53.

Lazzery, A., Bucknall, C.B., 1995. Application of a dilatation yielding model to rubber-toughened polymers. Polymer 36, 2895–2902.

McClintock, F.A., 1968. A criterion for ductile fracture by the growth of holes. J. Appl. Mech. 6, 363–371.

McClintock, F.A., Kaplan, S.M., Berg, C.A., 1966. Ductile fracture by hole growth in shear bends. Int. J. Fract. Mech. 2, 614–626.

Michler, G.H., 1993. Electron microscopy in polymer science. Appl. Spectrosc. Rev. 28, 327–384.

Muravin, D.K., Oshmyan, V.G., 1999. Simulation of particulate-filled composite deformation diagrams on the basis of a constitutive model for large plastic deformations of a polymer matrix. J. Macromol. Sci.-Phys. B 38, 749–758.

Oshmyan, V.G., Muravin, D.K., 1997. On the transition between microhomogeneous and crazelike mechanism of debonding in particulate composites. Compos. Sci. Technol. 57, 1167–1174.

Paul, D.R., Newman, S., 1978. Polymer Blends. Academic Press, New York.

Pukansky, B., Van Es, M., Maurer, F.H.J., Voros, G., 1994. Micromechanical deformation in particulate filled thermoplastics: volume strain measurements. J. Mater. Sci. 29, 2350–2358.

Pukansky, B., Maurer, F.H.J., Boode, J.-W., 1995. Impact testing of polypropylene blends and composites. Polym. Eng. Sci. 35, 1962–1971.

Toya, M., 1974. A crack along the interface of a circular inclusion embedded in an infinite solid. J. Mech. Phys. Solid 22, 325–348.

Vavakin, A.S., Salganik, R.A., 1975. On the effective characteristics of heterogeneous media with isolated inclusions. Izvestiya Akademii Nauk SSSR, Mekhanika Tverdogo Tela 3, 65–75.

Vollenberg, P.H.T., Heikens, D., 1989. Particle size dependence of the Young's modulus of filled polymers. 1. Preliminary experiments. Polymer 30, 1656–1662.

Vollenberg, P.H.T., de Haan, J.W., van de Ven, L.J.M., Heikens, D., 1989. Particle size dependence of the Young's modulus of filled polymers. 1. Annealing and solid-state nuclear magnetic resonance experiments. Polymer 30, 1663–1668.

Wong, F.C., Ait-Kadi, A., 1995. Mechanical behavior of particulate composites: experiments and mechanical predictions. J. Appl. Polym. Sci. 55, 263–278.

Wu, S., 1985. Phase structure and adhesion in polymer blends: a criterion for rubber toughening. Polymer 26, 1855–1863.

Wu, S., 1988. A generalized criterion for rubber toughening: the critical matrix ligament thickness. J. Appl. Polym. Sci. 35, 549–561.

Zhuk, A.V., Knunyantz, N.N., Oshmyan, V.G., Topolkaraev, V.A., Berlin, A.A., 1993a. Initiation and growth of interfacial defects in particulate filled polymer composites. Polym. Sci. 35, 1501–1512.

Zhuk, A.V., Knunyantz, N.N., Oshmyan, V.G., Topolkaraev, V.A., Berlin, A.A., 1993b. Debonding microprocesses and interface strength in particle filled polymer materials. J. Mater. Sci. 28, 4595–4606.

Zhuk, A.V., Knunyantz, N.N., Oshmyan, V.G., 1994. Transformation of adhesive cracks into cohesive ones in particulate-filled composites. Polym. Sci. 36, 694–698.